Performance characteristics of GaN/$Al_{0.2}Ga_{0.8}N$ quantum dot laser at $L = 100$ Å

H. Bouchenafa[a,*], B. Benichou[b,c], and B. Bouabdallah[c]
[a]*Department of Physics, Faculty of Science Exact and Informatics, Hassiba Ben Bouali University, Chlef 02000, Algeria.*
**e-mail: bouchenafa_halima@yahoo.fr*
[b]*Department of Electronics, Faculty of Technology, Hassiba Ben Bouali University, Chlef 02000, Algeria.*
[c]*Condensed Matter and sustainable Development Laboratory, Djillali Liabés University, Sidi Bel Abbés 22000, Algeria.*

Received 2 July 2018 ; accepted 1 October 2018

In this paper, a theoretical model is used to study the optical gain characteristics of GaN/$Al_{0.2}Ga_{0.8}N$ quantum dot lasers. The model is based on the density matrix theory of semiconductor lasers with relaxation broadening. The effect of doping varying the side lengths of the box in the structure is taken into account. A comparative study of the gain spectra of p-doped, undoped and n-doped structures of GaN cubic quantum-dot laser respectively, is presented for various side lengths. The variation of peak gain on carrier density is also presented. The effect of side length on the variation in modal gain versus current density is plotted too. The results indicate that the p type doping is efficient to reach a better optical gain value, and to achieve low threshold current densities compared with undoped and n-doped structures, and the optimum value for quantum dot width to achieve the lower threshold current density for the three cases is $L = 100$ Å.

Keywords: Quantum dot; optical gain; III-nitride semiconductors; laser threshold.

PACS: 85.35.Be; 78.67.Hc

1. Introduction

The semiconductor quantum dot active region takes full advantage of the quantum confinement effect. The three dimensional quantum confinement of carriers results in discrete carrier energy level structure in a quantum dot active region [1-3]. Consequently, the quantum dot laser diode offers the potential performance in high optical gain [1,2], low threshold current density [2,4] and high characteristic temperature [1].

The use of quantum dots in nitride semiconductors is more effective, since the zero-dimensional electronic states in the QDs play an essential role for improving optical gain and threshold current characteristics particularly in wide bandgap semiconductors.

III-nitride based devices are of particular interest due to their wide range of emission frequencies and their potential for high-power electronic applications [5]. The band gap energy ranges from 0.7 eV for InN, 3.4 eV for GaN to 6.2 eV for AlN [6]. By adding Indium and Aluminum to GaN, ternary alloys can be formed with wide bandgap range of from 0.7 to 6.2 eV, which can cover the spectral range from deep ultra violet (UV) to infrared (IR) at room temperature [7,8].

In this work, we analyze the optical gain and threshold performances of the GaN/$Al_{0.2}Ga_{0.8}N$ quantum dots lasers, based on the density matrix theory of semiconductor lasers with relaxation broadening [2] including the effect of doping and side length of quantum box.

The optical gain and threshold current density represent the basic elements that must be optimized to produce a high performance quantum box laser, and are also important elements in the study and comparison of the effect of p-type doping and n-type doping in GaN/$Al_{0.2}Ga_{0.8}N$.

2. Theoretical background

2.1. Optical Gain Theory

Taking into account the intraband relaxation in the same way as in Ref. [2], the optical gain of quantum box lasers active region is given by:

$$g(\omega) = \frac{\omega}{n_r}\sqrt{\frac{\mu_0}{\varepsilon_0}}\sum_{lmn}\int_{E_g}^{\infty}\langle R_{cv}^2\rangle \times \frac{g_{cv}(f_c - f_v)(\hbar/\tau_{in})}{(E_{cv} - \hbar\omega)^2 + (\hbar/\tau_{in})^2}dE_{ch} \quad (1)$$

Here the subscript c (or v) denotes the conduction band (or heavy- hole band), where f_c and f_v are the corresponding Fermi functions for electrons in the conduction and valence bands given by:

$$f_c = \frac{1}{1 + \exp(\varepsilon_{cn} - E_{fc})/kT}, \quad (2a)$$

$$f_v = \frac{1}{1 + \exp(\varepsilon_{vn} - E_{fv})/kT}. \quad (2b)$$

Where ε_{cn} et ε_{vn} are the total energies of electrons and holes for subbands n.

E_{cv} is a transition energy between the conduction band and valence band, R_{cv} is the dipole moment, ω is the angular frequency of light, ε_0 and μ_0 are the dielectric constant and permeability of the vacuum, τ_{in} the intraband relaxation

time ($\tau_{in} = 0.1$ ps), n_r is the refractive index and g_{cv} is the density of states for the QD, given by [2]:

$$g_{cv}(E_{cv}) = \frac{2\delta(E_{cv} - E_{cnml} - E_{vnml}E_g)}{L_x L_y L_z}. \quad (3)$$

Where $\delta(E)$ is the delta function, and E_{cnml} and E_{vnml} are the quantized electron and hole energy levels respectively of a quantum box structure in x, y and z directions, respectively [9]. If we assume a structure consisting of GaN/$Al_{0.2}Ga_{0.8}$N quantum box with a dimension of L_x, L_y and L_z, energy levels are expressed by the following equation, where the barrier height in the potential profile is assumed to be infinite [10]:

$$E_{cnml} = \frac{\hbar^2}{2m_c^*}\left(\left(\frac{n\pi}{L_x}\right)^2 + \left(\frac{m\pi}{L_y}\right)^2 + \left(\frac{l\pi}{L_z}\right)^2\right) \quad (4a)$$

$$E_{vnml} = \frac{\hbar^2}{2m_v^*}\left(\left(\frac{n\pi}{L_x}\right)^2 + \left(\frac{m\pi}{L_y}\right)^2 + \left(\frac{l\pi}{L_z}\right)^2\right) \quad (4b)$$

Where m_c^* and m_v^* are the effective masses of an electron and hole respectively, n, m and l denote the label of the quantized energy levels in the box.

In Eq. (1), we have supposed that the electron and hole in the quantum box are in equilibrium determined by the quasi-Fermi levels E_{fc} and E_{fv} respectively.

E_{fc} and E_{fv} are related to the electron and hole densities injected into the quantum box as [2,7]:

$$N = \sum_{nml} \frac{2}{\left[1 + \exp\left(\frac{E_{cnml} - E_{fc}}{kT}\right)\right] L_x L_y L_z}, \quad (5a)$$

$$P = \sum_{nml} \frac{2}{\left[1 + \exp\left(\frac{E_{fc} - E_{vnml}}{kT}\right)\right] L_x L_y L_z}. \quad (5b)$$

In the approach of Eqs. (1), (5a) and (5b), we have assumed the transition from the first conduction band to the first valence band (heavy hole band) because the density of states of light hole band is smaller than that of the heavy hole band and it's probability to occur is more significant than of the other transitions .

2.2. Effects of impurities doping

The presence of donors or acceptors can be accounted by replacing N in Eq. (5a) by $N + N_d$ and N in Eq. (5b) by $N + N_a$.

Where N_d and N_a are the donor and acceptor densities respectively [10,11].

2.3. Threshold current density

The threshold carrier density is calculated using the following equation [12]:

$$N_{th} = N_{tr} + \frac{1}{\Gamma a}\left(\alpha_i + \frac{1}{2L_c}\ln\left(\frac{1}{R}\right)\right). \quad (6)$$

Where α_i is internal loss, a is differential gain, Γ is optical confinement factor, L_c is cavity length and N_{tr} is transparency carrier density.

The threshold current density using threshold carrier density (N_{th}) is written as [2,14,15]:

$$J_{th} = \frac{n\eta q L_z N_{th}}{\tau_s}. \quad (7)$$

Where q is electron charge, η is the rate of surface area of quantum boxes included in the whole area, n is the number of the layers of quantum box array and τ_s is carrier life time.

3. Results and discussion

It's assumed that the quantum dot structure studied has a GaN in the form of cubic active layer of L side length ($L = L_x = L_y = L_z$) sandwiched between $Al_{0.2}Ga_{0.8}N$ barriers (Fig. 1), using quantum box model we calculate quantum dot quantized energy levels for conduction and valence bands which are implemented in the model described above to calculate the optical gain . The parameters used in calculation are listed in Table I.

Figure 2 presents a comparison between optical gain spectra of undoped structure for GaN quantum dot and p-doped structure with acceptor densities $N_a = 5 \times 10^{18}$ cm^{-3}

TABLE I. The parameters used in the calculations (m_0 is the free electron mass)

	GaN	AlN
Band gap energy(E_g(eV))	3.43	6.2
Electron effective mass(m_e)	0.2 m_0	0.3 m_0
Heavy hole effective mass(m_{hh})	0.8 m_0	1.14 m_0
refractive index n_r	2.67	2.03
Spin orbit splitting Δ_{cr} (eV)	0.019	-0.164

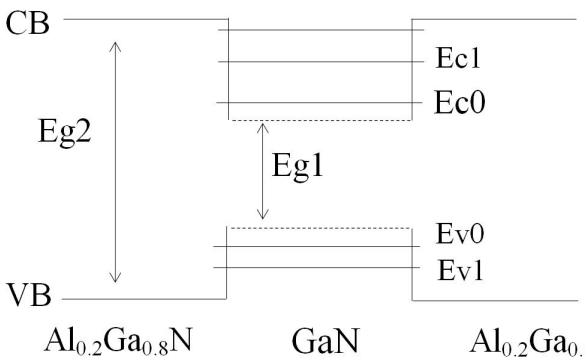

FIGURE 1. One-dimensional scheme of the band diagram of GaN based quantum dot. CB: conduction band; VB: valence band; Eg1: band gap of GaN; Eg2: band gap of $Al_{0.2}Ga_{0.8}N$, Ec0/Ev0 are ground quantized energy levels of electron and hole in CB and BV respectively.

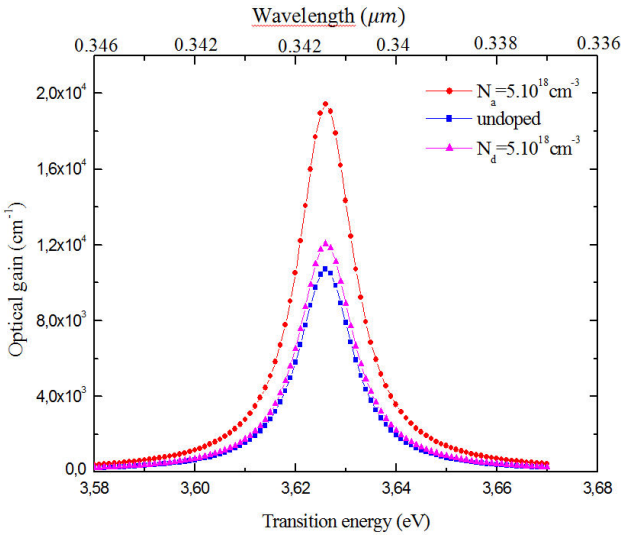

FIGURE 2. Optical gain versus transition energy of undoped structure compared with gain spectra of p-doping ($N_a = 5 \times 10^{18}$ cm^{-3}) and n-doping ($N_d = 5 \times 10^{18}$ cm^{-3}) for GaN/$Al_{0.2}Ga_{0.8}N$ quantum dot laser at $L = 60$ Å, $N_v = 2 \times 10^{19}$ cm^{-3}.

and n-doped structure with donor densities $N_d = 5 \times 10^{18}$ cm^{-3} at side length of quantum dot $L = 60$ Å and injection carrier $N_v = 2 \times 10^{19}$ cm^{-3}, where we observed a higher optical gain value in p-doped structure than that in undoped or n-doped structure.

The p-type doping effectively decreases f_v since N is increased to $N + N_a$, causing an increase in $f_c - f_v$. On the other hand, n-type doping does not give rise to significant increase in $f_c - f_v$ when N is increased to $N + N_d$.

In Fig. 3, the optical gain is plotted as function of the photon energy for various side length of a cubic quantum box for p-doped, undoped and n-doped structures respectively; it is observed that the gain is higher at $L = 60$ Å for both cases due to the increase of carrier density for population inversion in small size quantum box. On the other hand, when the size of the quantum dot increases, the carriers in the box are distributed over useless levels, and the separation between energy levels is not enough to obtain high gain. It should also be noted that the p-doped structure has the best value of maximum gain compared to the other structures.

Figure 4 shows the high sensitivity of maximum gain to changes in carrier density for different values of quantum box's size of p-doped, undoped and N-doped structures respectively.

It shows also for both cases, two regions (positive side) and absorption (negative side) and that give us the value of the transparency density N_{tr} from which the material begins to amplify the photon whose energy satisfies the conduction of Bernard-Duraffourg ($E_g < h\nu < E_{fc} - E_{fv}$) for each box size (where $h\nu$ is photon energy).

The modal gain is also a fundamental characteristic for lasing action in hetero-structures. It is obtained by multiplying optical gain with confinement factor. When the modal gain overcomes the total loss, the lasing action takes place. It is expressed as: $g_m = \Gamma \cdot g$ where Γ is optical confinement factor.

The variation of modal gain on current density values for different sizes of quantum box of three structures p-doped,

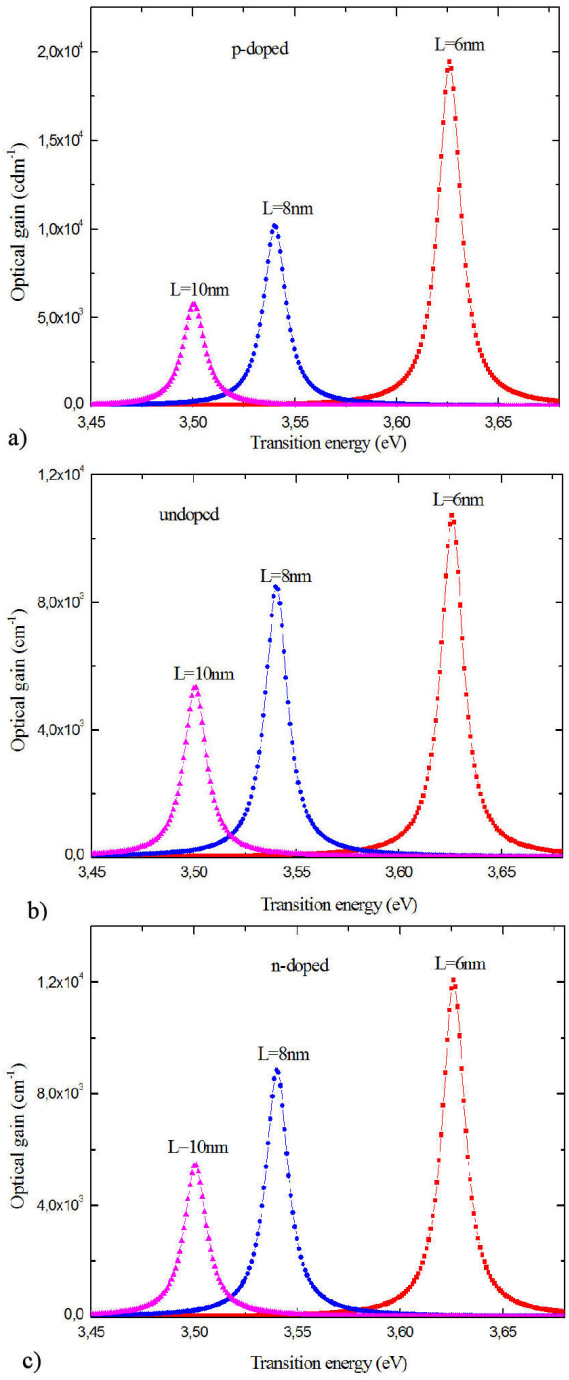

FIGURE 3. Gain spectra of p-doped ($N_a = 5 \times 10^{18}$ cm^{-3}), unpoded and n-doped ($N_d = 5 \times 10^{18}$ cm^{-3}) for GaN quantum dot laser for different sizes of quantum box at $N_v = 2 \times 10^{19}$ cm^{-3}.

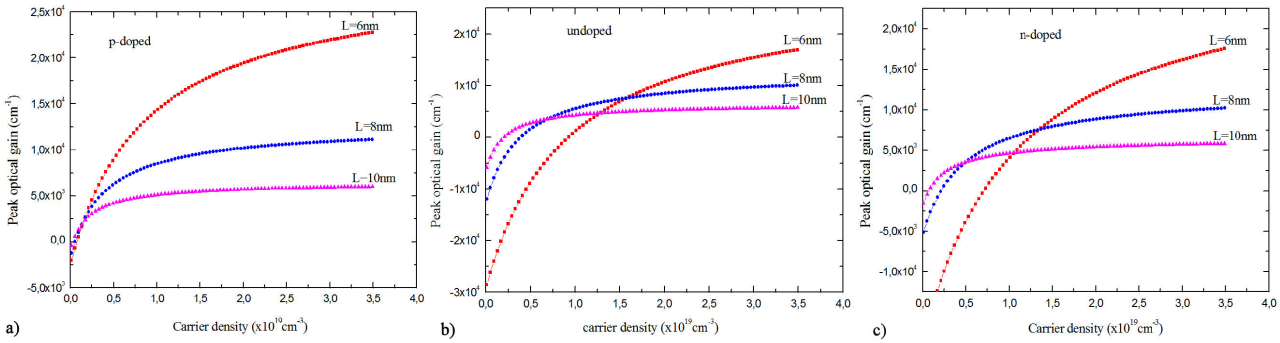

FIGURE 4. Dependence of peak optical gain on carrier density in GaN QD of p-doped ($N_a = 5 \times 10^{18}$ cm^{-3}), unpoded and n-doped ($N_d = 5 \times 10^{18}$ cm^{-3}) structures for different sizes of quantum box at $N_v = 2 \times 10^{19}$ cm^{-3}.

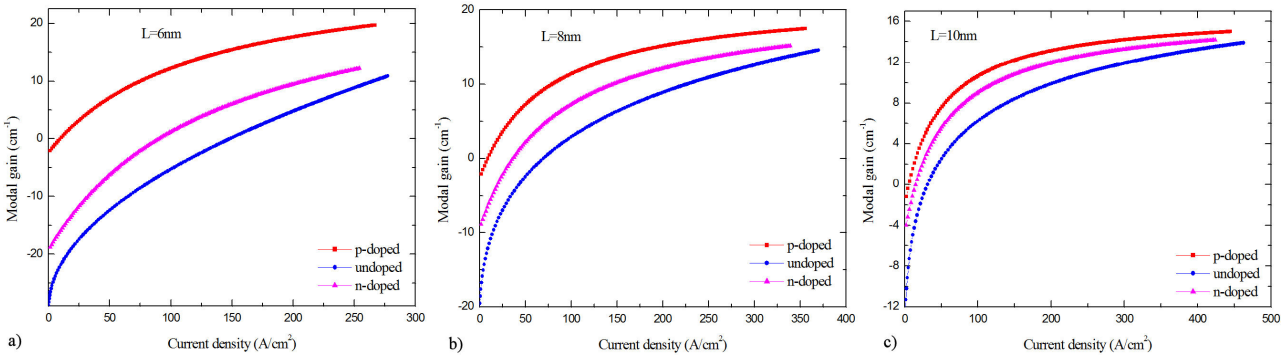

FIGURE 5. Modal gain as function of current density for GaN/Al$_{0.2}$Ga$_{0.8}$N QD structure for different sizes of quantum box of p-doped ($N_a = 5 \times 10^{18}$ cm^{-3}), unpoded and n-doped ($N_d = 5 \times 10^{18}$ cm^{-3}) structures at $N_v = 2 \times 10^{19}$ cm^{-3}.

TABLE II. Performance characteristics of GaN/Al$_{0.2}$Ga$_{0.8}$N QD structure for different sizes of cubic quantum box of p-doped ($N_a = 5 \times 10^{18}$ cm^{-3}), unpoded and n-doped ($N_d = 5 \times 10^{18}$ cm^{-3}) structures at $N_v = 2 \times 10^{19}$ cm^{-3}.

	p-doped			undoped			n-doped		
Side length (Å)	60	80	100	60	80	100	60	80	100
Gain max (cm^{-1})	19545	10483	5897	10909	8608	5420	12500	8948	5478
Transition energy (eV)	3.626	3.54	3.5012	3.626	3.54	3.5012	3.626	3.54	3.5012
Peak wavelenght(nm)	342	350	354	342	350	354	342	350	354
Emission spectrum	UV	UV	UV	UV	UV	UV	UV	UV	UV
N$_{tr}$ ($\times 10^{19}$ cm^{-3})	0.073	0.06	0.019	0.926	0.391	0.2	0.71	0.215	0.075
Transparency current J$_{tr}$ (A/cm^2)	9.35	8.83	6.72	148.37	69.67	33.4	91.1	37.57	15.58
Threshold current density J$_{th}$ (A/cm^2)	56.68	56.2	52.38	237	178.1	136	176	108	78.3

undoped and n-doped is plotted in Fig. 5. This last figure is particularly useful because it shows the interrelation among the three parameters of interest: gain modal, current and side of length of QD, and allows immediate comparison between different quantum dots.

From this figure: we observe a parabolic increase for initial values of the current density but it saturates afterwards indicating very small or negligible increase in modal gain with change in current density, we note also, that the transparency current density J_{tr} (intercept at gain =0), which is the value at which the active layer neither absorbs nor amplifies the light at the lasing wavelength, decreases with increasing of the side length of quantum box. Moreover, the slope of the gain versus current density plot decreases with increasing of the side length of quantum box.

For laser oscillation, the modal gain must equal the total losses α_{total}. The laser oscillation condition is given as [16,17,18]:

$$G_{mod} = \Gamma g_{th} = \alpha_i + \frac{1}{2L_c} \ln\left(\frac{1}{R}\right) = \alpha_{\text{total}}. \qquad (8)$$

Assuming that $\alpha_i = 5$ cm^{-1}, $R = 0.3$, $n = 1$ and $L_c = 4.2$ mm, the threshold current density J_{th} that corresponds to the modal gain value that satisfies the oscillation

condition can be obtained from the modal gain-current density plots [19,20].

From these curves and Table II summarizing the results, we can deduce that the p-type doping makes it possible to increase the gain peak and to reach an emission threshold for low carrier concentrations relative to the undoped or n-doped case, which makes it possible to achieve at minimum values of threshold current densities, and that the optimum size of the cube for lowest threshold is shifted to longer length of the side because low gain can be achieved without carrier injection for the useless levels. Which gives that the optimal structure is p-doped structure with $L = 100$ Å, the value of the gain is 5897 cm^{-1} and the minimum value of threshold current density is about 52.38 A/cm^2.

4. Conclusion

In this paper, we have investigated the optical gain characteristics of $GaN/Al_{0.2}Ga_{0.8}N$ quantum dot laser and the effect of doping and size of quantum dot on its performance. We have presented also the modal gain characteristics of $GaN/Al_{0.2}Ga_{0.8}N$ QD for both structures. The variation in modal gain with increasing current density has been plotted with the effect different sizes of quantum box. The following findings can be stated: the effect of p-doping is efficient by increasing gain; n-doping has less effect and gain increases with reducing quantum box size. The results indicate also that better performance can be achieved with $GaN/Al_{0.2}Ga_{0.8}N$ p-doped quantum dot laser with $L = 100$ Åcompared to undoped and n-doped structure.

1. Y. Arakawa, and H. Sasaki, *App. Phys Lett*. **40** (1982) 939.
2. M. Asada, Y. Miyamoto, and Y. Suematsu, *IEEE J. Quantum Electron*. **22** (1986) 1915.
3. K. Vahala, *IEEE J. Quantum Electron*. **24** (1988) 523.
4. Y. Arakawa, A. Yariv, *IEEE J. Quantum Electron*. **22** (1986) 1887.
5. N. Baer *et al*., arXiv: con- mat/0509545v1 [cond-mat.other] (2005).
6. M. Miyamura, K. Tachibana, and Y. Arakawa, *Phys. Stat. sol. (a)* **192** (2002) 33.
7. K. H. Al-Mossawi, *Opt Photonics J.* **1** (2011) 65.
8. S. Nakamura *et al*., *Jpn. J. Appl. Phys.* **36** (1997) L1568.
9. E.O. Chukwuocha, and M. C. Onyeaju, *Int. J. Scientific. Technol. Res.* **1** (2012) 21.
10. P. Harrison, *Quantum Wells*, Wires and Dots, 2nd ed. (John Wiley & Sons, 2005), pp. 243-270
11. K.J. Vahala, and C.E.Zah, *App. Phys Lett*. **52** (1988) 1945.
12. M.Toshihko, *IEEE J. Quantum Electron.* **32** (1996) 493.
13. H.K. Choi, C.A. Wang, and S.j. Eglash, *The lincoln laboratory journal*. **3** (1990) 395.
14. M. Sugawara, *Self Assembled* InGaAs/GaAs *Quantum dots* 1st ed. (Academic Press, 1999), pp. 246-247.
15. D.G. Deppe, K. Shavritranuruk ,G. Ozgur, H. Chen and S. Freinsem, *Electronics Letters*. **45** (2009) 54.
16. G. L.Su, T. Frost, P. Bhattacharya, J. M. Dallesasse, and S.L. Chuang, *Optics express.* **22** (2014) 22716.
17. M. Sharma, R. Yadav, P. Lal, F. Rahman, and P. A. Alvi, *Advances in Microelectronic Engineering (AIME)*. **2** (2014) 27.
18. Z. A. Thaira, and J. M. Sahan, *IJORT*. **3** (2014) 94.
19. F. Hadjaj, A. Belghachi, and A. Helmaoui, *Sensors & Transducers*. **192** (2015) 90.
20. Q. Lu, Q. Zhuang, and A. Krier, *Photonics*. **2** (2015) 414.